Received: 27 September 2022 | Revised: 23 February 2023 | Accepted: 2 April 2023
DOI: 10.1002/ep.14148

ENVIRONMENTAL PROGRESS & SUSTAINABLE ENERGY

ORIGINAL RESEARCH

Sustainable Energy

Solar photovoltaic water pump performance optimization by using response surface methodology

Vipan Chand Waila[1] | Abhishek Sharma[2] | Vineet Singh[3] | Naveen Kumar Gupta[4]

[1]School of Science and Technology, Glocal University, Saharanpur, India

[2]Department of Mechanical Engineering, G L Bajaj Institute of Technology and Management, Greater Noida, India

[3]Department of Mechanical Engineering, School of Engineering & Technology, IFTM University, Moradabad, India

[4]Department of Mechanical Engineering, Institute of Engineering and Technology, GLA University, Mathura, India

Correspondence
Abhishek Sharma, Department of Mechanical Engineering, G L Bajaj Institute of Technology and Management, Greater Noida, India.
Email: absk2001@gmail.com

Abstract

The constant depletion of the existing energy sources and their environmental effects have generated interest in employing renewable energy sources to power water pumping systems, such as solar-photovoltaic. The research addresses the optimal photovoltaic (PV) power output, solar radiation, operating head, and tilt angle for maximum solar energy used to capture more solar radiation for solar water pumping for irrigation purposes. In order to get the best performance from the solar PV water pump, such as discharge (Q), hydraulic power (P_H), pump efficiency ($\acute{\eta}_p$), and overall efficiency ($\acute{\eta}_o$), the design of experiments-based response surface methodology was implemented in this work. The data required for the RSM model were obtained from the experimental work performed at location 28.67° N, 77.21° E, Delhi, India. The experiments performed at five different ranges of input variables PV power output (4000, 4250, 4500, 4750, and 5000 W), Solar radiation (200, 350, 500, 650, and 800 W/m^2), operating head (15, 20, 25, 30, and 35 m) Tilt angle (5°, 10°, 15°, 20°, and 25°). The best output parameters The best conditions for a solar PV water pump (16.8 m3/h discharge, 1.85 kW hydraulic power, 81.15% pump efficiency, and 16.12% overall efficiency) were discovered to be P_o 5000 W, SA 260 W/m^2, Head 35 m, and TA 19°. The predicted result was validated using an RSM-based solution, and the error% was found to be within acceptable limits (>5%). The desirability 0.963 of the model was indicating the good solution.

KEYWORDS
response surface methodology, solar photovoltaic water pump system, solar radiation, tilt angle

1 | INTRODUCTION

Agriculture contributes significantly to a country's GDP growth such as India, where around 70% of the whole population is directly involved in agriculture, which has resulted in a steady increase in energy consumption over the previous few years. Water is essential for irrigation in order to run the agriculture sector efficiently. Furthermore, the amount and quality of accessible water resources in every country strongly influence the quality of life of a country. Although there is a lot of high-quality water around the globe, it is not always available in places where it may be used. This increases the requirement for high-quality water to be pumped from its source to places where it is needed. Water pumps have been used for this purpose for decades.[1]

The population of the Indian subcontinent uses water pumping which is often powered by conventional electricity or diesel-generated energy to pump water from wells and rivers. The usage of diesel-powered water pumping equipment not only necessitates the use of expensive fuels but also causes noise and air pollution, notably the emission of greenhouse gases such as carbon dioxide (CO_2) into the atmosphere.[2] The typical pumping system has the benefit of being simple to install, but it has several drawbacks, including regular equipment repair, refueling, and limited reserves of diesel.[3]

Therefore, as researchers grew more aware of the damaging effects of burning fossil fuels on the environment, they increased their efforts to create autonomous water pumping devices that could be driven by renewable energy. Solar energy, wind energy, producer gas, and biogas are the four potential renewable energy sources that might be utilized to pump water.[4] Crops need a lot of water throughout months and days of sunshine. Solar energy has a huge potential for powering water pumps in countries like India, where there are more than 300 sunny days a year.[5] As a result, among renewable energy sources, solar energy is suitable for pumping water in agriculture since the time of day when it is accessible corresponds to when most crops require water. Furthermore, since most rural, arid, and isolated areas in poor nations are not linked to electric networks, solar energy-based irrigation is a more dependable and practical choice for irrigation farms.[6,7]

The nature of solar power generation systems is consistent. They produced no hazardous by-products. They are not mined from the earth's strata and emit no hazardous pollutants into the environment.[8,9] PV pumping is one of the most prospective uses of solar energy systems since it is environmentally beneficial, requires little maintenance, and has no fuel costs.[10] The technique is comparable to any other conventional water pumping system, with the exception that it is powered by solar energy. The pumped water flow rate is determined by incident solar energy and the size of the PV array.[11] When compared to conventional pumping systems, a well-built PV system results in significant long-term cost savings. Tanks can also be used for water storage rather than batteries for power storage.[12] Solar photovoltaic (PV) panels immediately convert sunlight into useable electrical energy, which may then be used to power a water pump directly or via an inverter. Solar PV water pumps are made up of many components that can be classified as mechanical, electrical, or electronic. These components differ in their manufacture, operation, and performance. The integration and synchronization of such a diverse set of components to build a system, such as a solar PV water pump, is challenging to operate and results in overall poor performance. Furthermore, the system's engagement with multidisciplinary and advanced technology necessitates a wide range of technical knowledge for its operation and maintenance.[13–15]

Allouhi et al.[16] investigated an optimized PV system configuration capable of supplying a solar submersible pump system to meet the domestic water needs of five isolated houses in a remote Moroccan area and discovered that the appropriate design and smooth operation are primarily dependent on available solar irradiation, domestic water demand, and the proposed system's appropriate configuration. The results showed that the second system, which used an MPPT DC converter and fewer PV arrays, could pump more water and outperformed the direct connection arrangement substantially. Mustapha Errouha et al.[17] attempted to build a simple and low-cost photovoltaic (PV) water pumping system (PVWPS) design employing a high-efficiency induction motor. The suggested PV system is built of two stages of converters which the first one assures the highest power point by adjusting the duty ratio of boost converter using variable step size incremental conductance (VSS INC) approach. The simulation results reveal that the proposed PVWPS performed best in terms of the time of reaction; pumped water, flux ripples, and the stator currents are minimized. S. Senthil Kumar et al.[18] proposed the most effective way for conserving power and water. The sprinkler with solar water pump is used in a water irrigation system to reduce water usage and power consumption. The sprinkler is used to spray water in an irrigation field in order to reduce water use. The PV technology utilized for creating power is used to run the motor used for solar pump. The combination sprinkler and ecologically friendly and cost-effective PV technology helps to limit the utilization of power and water. Verma et al.[19] gave a brief summary of the solar PV-powered water pumping system, including its key components, applications, and India context. Economic and environmental concerns were also raised. In compared to diesel-powered water pumps, solar PV water pumping systems are shown to be more cheap, eco-friendly, dependable, with fewer maintenance and a longer life duration. Some of the systems have a payback period of 4–6 years. The new Indian subsidy offered and the latest scheme accessible for installation reasons is also mentioned in the study. Tiwari and Kalamkar et al.[20] conducted an experimental study to determine how PV designs, total head, and solar radiation affect PV pumping system performance. Abhilash et al.[21] created a silicon PV tracking-based pumping device that uses solar energy for irrigation. The pump's size was certified based on motor power. It was discovered that the size varies depending on the output and height of the pump used to draw water. Efficiency grows in lockstep with size. It was also said that silicon material as a solar panel is the main structure for increasing efficiency and lowering costs. Tomar[22] designed cooperative irrigation-based PVWP (CI-PVWP) system demonstrates the advantages of enhanced PV use throughout the morning and evening hours. It allows farmers to utilize the PV for water pumping cooperatively during the morning/evening hours when available PV power is typically less than the minimum operational power consumption of the motor-pump system. Primary simulation findings show higher PV energy usage during morning/evening hours and assure MPPT functioning. Waila et al.[23] used the RSM technique to investigate the impacts of AT (°C), SR (W/m^2), SAA (degrees), and TA (degrees) on SPVWPS. The RSM was used to model to find optimal values of input parameters in order to optimize the output response discharge (m^3/h) and pump efficiency (%). Maximum discharge (48.7 m^3/h) and pumping efficiency (58.8%) are achieved for a parameter combination of solar radiation (451 W/m^2), ambient temperature (27°C), surface azimuthal angle (−18°), and tilt angle (55°). It was discovered that the mathematical model developed could properly forecast the performance and efficiency of the SPVWPS.

Additionally, according to the researchers, the performance of PV modules is highly impacted by solar cell temperature, solar irradiation intensity, and the mass flow rate of cooling fluids, humidity, and dust. Environmental considerations, the caliber of the PV panels, and the functionality of the controller, energy storage unit, pump, and motor are the main variables that determine the performance and efficiency of SPVWPS. Irradiance and temperature variations have an impact on the SPVWPS's water production and ideal size of the solar panel and pump. The goal of this research is to examine how various environmental factors, including solar radiation, PV power output, operating head, and tilt angle, affect the efficiency of solar PV pumps. Moreover, the efficiency of a solar-powered pump on an irrigation system was examined and tested by adjusting the aforementioned input parameters. Improve the ideal parameter, such as discharge, hydraulic power, pump efficiency, and overall efficiency, to improve the performance of a solar-powered pump. The use of response surface methodology to optimize the input variables in order to maximize the performance of the solar pump is a novel aspect of this work. A number of modeling equations and approaches have been developed utilizing the RSM-based CCD model to optimize PV system performance. The estimated result is then confirmed, and the error is determined.

The solar Pump performance mainly depends on the four parameters. The Three parameters tilt angle, surface azimuth angle and module temperature govern the efficiency of the solar pump and the speed of the pump control the efficiency of the pump. So, in this research article, the overall performance has been optimized by the four input variables by RSM. This method is novel and new since the optimum setting of these four input variables maximizes the overall efficiency of solar panels.

2 | SOLAR PV WATER PUMPING METHODOLOGY

2.1 | Working principle of solar PV water pump

The SPVWPS system combines a solar panel with a pump, with the pump being powered by energy produced by the PV panel. The PV cell, which directly transforms solar energy from sunlight into electrical energy, is the fundamental functioning component. The PV panels are coupled with an electric motor (either DC or AC), which transforms the electrical energy from the PV panel into mechanical energy, which is then transformed into hydraulic energy by the pump. This system may also employ storage components like a battery to store electric charge and a reservoir to store water. The pump's required head and discharge vary depending on the application. A suitable pump and photovoltaic panel are used based on the required head and discharge. The capacity of a solar pumping system to pump water is determined by three major variables: pressure, flow, and pump power. Pressure may be thought of as the labor done by a pump to move a given amount of water up to the storage tank for design reasons. The amount of work required by a pump is determined by the elevation difference between the water source and the storage tank. Figure 1 is a schematic of a typical solar photovoltaic water pumping system. In the experimental setup, a controller has been used in place of inverter. The controller converts the DC current into the AC current as per the requirement of the motor current and voltage. The controller also has the display system inbuilt in it, which shows the current, voltage, head developed, discharge and RPM of the solar pump. The solar flux separately measured by the pyranometer.

2.2 | Theoretical analysis

2.2.1 | PV power output (P_o) of the solar PV modules[24]

$$P_o(W) = V_o \times I_o, \tag{1}$$

where V_o is the operating voltage (V) and I_o is the operating current (A) of PV panel.

Figure 2 shows the energy input and output over the solar plate, here minor losses like reflection, absorption of solar radiation, resistance losses occur in the solar cell have been neglected. So according to the first law of thermodynamics.

$$Q_{in} = V_m I_m + Q_{heat}. \tag{2}$$

Now, first law of efficiency of solar panels.[9]

$$\eta_{cell} = \frac{V_m I_m}{Q_{in}}. \tag{3}$$

2.2.2 | Hydraulic power (P_H)[24]

$$P_H(\mathrm{kW}) = \frac{\rho \times g \times Q \times H}{3.6 \times 10^{-6}}, \tag{4}$$

where ρ is the density of water (1000 kg/m^3), g is the acceleration due to gravity (9.81 m/s^2), Q is the discharge through pump (m^3/h), and H is the operating head (m).

The head developed by the pump is given by following equation presented in Reference 10.

$$H = H_{St} + \frac{(f + \Sigma K)V^2}{2g}, \tag{5}$$

where H_{st} is the static head (m), f is the friction factor, ΣK is the sum of minor head loss factor, and g is the gravitational acceleration (m/s^2).

Pump efficiency ($\acute{\eta}_p$)[24]

$$\text{Pump efficiency}\,(\%) = \frac{\text{Hydraulic power required by the pump (kW)}}{\text{Power required for the motors (kW)}} \times 100. \tag{6}$$

Overall efficiency ($\acute{\eta}_o$)[24]

$$\text{Overall efficiency} = \acute{\eta}_{pump} \times \acute{\eta}_{panel}, \tag{7}$$

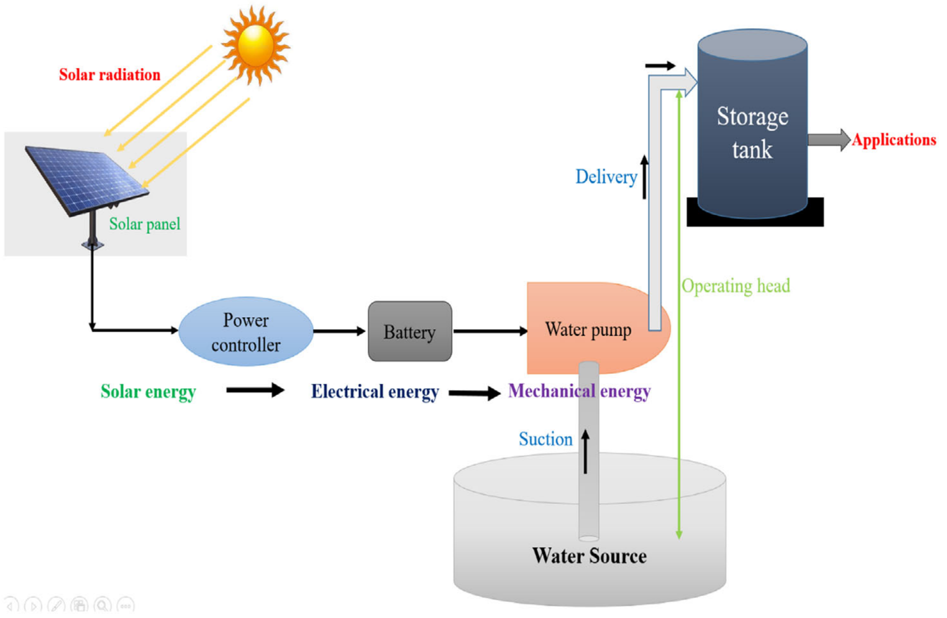

FIGURE 1 Process of a solar-powered water pump system.

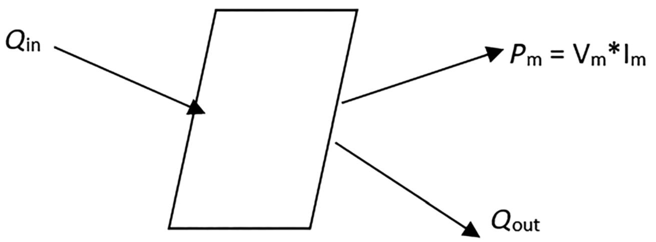

FIGURE 2 Solar panel energy balance.

$$\acute{\eta}_{\text{pump}} = \frac{\rho g Q H}{FF I_{SC} V_{OC}}, \tag{8}$$

where ρ is the density of water, Q is the discharge of water (m^3/s), FF is the fill factor (0.88) provided by the manufacturer, I_{SC} is the short circuit current (amp), and V_{OC} is the open circuit voltage (V).

The solar panel efficiency is given by following Equation (9).

$$\acute{\eta}_{panel} = \frac{FF I_{SC} V_{OC}}{I_t A_P n}. \tag{9}$$

Time required for filling the tank has been calculated by following equations.[24]

$$\text{Time}\,(t) = \frac{\text{Volume of tank}}{\text{Discharge}}. \tag{10}$$

2.2.3 | Total number of solar panels and battery required

The total number of solar panels required for supply of required discharge given by following equation.[24]

$$N_P = \frac{\rho g Q H}{\eta_P \eta_B \eta_M T I_t A}, \tag{11}$$

where N_P is the total number of solar panels, η_P, η_B, and η_M is the solar panel efficiency, battery efficiency and the motor efficiency. T is the time for working of battery and It is the solar flux and A is the area of one solar panel.

The number of panel in series presented in Reference24.

$$N_S = \frac{V_R}{V_P}, \tag{12}$$

where V_R is the voltage required in motor and V_P is the voltage generated by single panel.

Number of panels in parallel is given by the following equation.[24]

$$N_P = \frac{N}{N_s}, \tag{13}$$

where N_P is number of solar panel in parallel number of batteries.[17]

$$N_B = \frac{T_B P_m}{(BAH) V_B}, \tag{14}$$

where N_B is the number of batteries, T_B is the time of working of batteries, BAH is the battery ampere hour, and V_B is the volt of battery.

2.2.4 | Solar cell modeling

Figure 3 represents the solar cell electric circuit representation. The solar cell current, voltage depends on the temperature and solar flux of the solar cell. The circuit consists of diode current I_{diode}, series

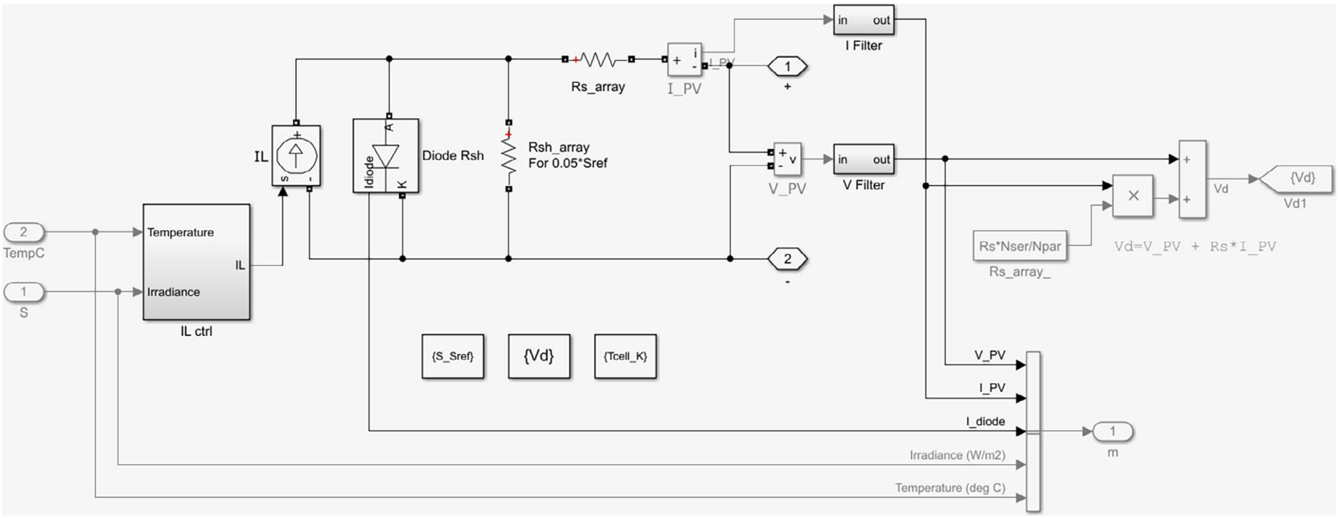

FIGURE 3 Solar cell electric circuit representation.

resistance Rs, photocurrent I_L, I_{SH} is a shunt, and I_{PV} is the total current (load current). Now by Kirchhoff's law.[20]

$$I_L = I_{PV} + I_{diode} + I_{SH}, \tag{15}$$

$$I_{PV} = I_L - I_{diode} - I_{SH}, \tag{16}$$

where I_{diode}, I_{SH} is the diode current and shunt current given by Tiwari and Kalamkar's[20] book of photovoltaic system engineering.

$$I_{diode} = I_o\left[e^{\left(\frac{eV}{kT}\right)} - 1\right], \tag{17}$$

$$I_{SH} = \frac{V + IR_S}{R_{SH}}. \tag{18}$$

Now

$$I_{PV} = I_L - I_o\left[e^{\left(\frac{eV}{kT}\right)} - 1\right] - \frac{V + IR_S}{R_{SH}}, \tag{19}$$

where I_o is represented in terms of open-circuit voltage as follows[20]:

$$I_o = I_L e^{-}\left(\frac{eV_{oc}}{kT}\right), \tag{20}$$

where V_{oc} is the (OCV), k is the BC, and T is the AT.

2.3 | Materials component and location

Table 1 shows the location of the system installation and the water resource. Table 2 depicts the material components required for the creation of a solar-powered submersible pump system in agriculture, which includes a variety of components and requirements. Table 3 contains extensive information on PV cells and PV arrays.

TABLE 1 Location and water resource information.

Name of location for system installation	New Delhi
Latitude	28.6448
Longitude	77.216721
Type of water resource	Deep well to storage
Application	Irrigation
Well diameter	80 cm
Static head	10 m
Maximum pumping depth	40 m

3 | RESPONSE SURFACE METHODOLOGY MODELING

3.1 | RSM Design matrix

The response surface method (RSM) is a statistical test method that is used to optimize random processes. RSM is made up of statistical approaches that have been used successfully to conduct experiments, build models, analyze the impacts of components, and discover the optimal conditions of factors for required replies.[25] One of the most significant advantages of RSM is that it reduces the number of experimental investigations necessary to collect enough information for statistically acceptable findings. Experiments were designed using MINITAB20. The response surface approach was used in this study to optimize the input variables PV power output, solar radiation, operating head, and tilt angle in order to increase the experiment's efficiency and cost-effectiveness.[26]

It employs experimental designs such as the central composite design (CCD), which fits the least-squares approach of RSM and is an

TABLE 2 Pumping system details.

Type of pump	Reciprocating pump
Type of motor	DC motor
Volume of storage tank	50 m^3
Height	5 m
Size of pipe	1

TABLE 3 Information about PV array.

Number of PV module	34
Number of module in series	6
Number of module in parallel	2
Power rating of per unit module	150 W
Maximum voltage rating	40 V
Maximum current rating	3.75 A
Total power capacity of PV array	5000 W

efficient method for process optimization. A regression equation can be generated by fitting the functional connection between the design factors and the response index. To maximize the response indices, a quadratic term is introduced to the equation. A total of 31 experiments were carried out in RSM using the quadratic model (Equation 21).[27]

$$Y = a_o + \sum_{i=1}^{k} a_i x_i + \sum_{i=1}^{k} a_{ii} x_i^2 + \sum_{i=1}^{k-1} \sum_{j=1}^{k} a_{ij} x_i x_j + \varepsilon, \tag{21}$$

where Y denotes the dependent parameters for the independent inputs, X_i is the main factor, and a_o, a_i, a_{ii}, and a_{ij} are constant coefficients of intercept, linear, quadratic, and interaction terms.

The input parameters have five coded values -2, -1, 0, $+1$, and $+2$ levels have been shown in Table 4. The 31 experiment array matrix is shown in Table 5.

3.2 | Model analysis

The importance of each parameter within the predetermined range for the various input parameters was ascertained using the analysis of variance (ANOVA) method. The analysis of variance for P_o, SA, H, and TA is presented in Tables 6 and 7. The F-value is used to evaluate the model's precision. The model is valid and the design factors significantly affect the response indices if the p-value is less than 0.05.[28] It was observed from the table that the P-value of P_o, head and tilt angle is less than 0.05 for all output responses. It signifies that these input parameters have a more significant effect on their corresponding output responses. In our findings, the experimental values' R^2 values were higher, showing that our model suited the data the best. The little difference between R^2 and modified R^2 allows for the creation of a more suitable statistical model. These numbers suggest that the quality of fit and prediction performance of each quadratic model is adequate. The summary statistic provides excellent justification for using quadratic models. Based on the CCD's numerical findings, quadratic regression models were created, and the fitted models are shown below (Equations 22–25).[29,30]

$$\begin{aligned} Q(\mathrm{m^3/h}) = {} & 76.6 - 0.0088\,P_o(\mathrm{W}) - 0.1097\,SA\left(\frac{\mathrm{W}}{\mathrm{m^2}}\right) - 0.02\,H(\mathrm{m}) \\ & - 1.64\,TA(\mathrm{degree}) - 0.000001\,P_o(\mathrm{W}) \times P_o(\mathrm{W}) \\ & + 0.000037\,SA\left(\frac{\mathrm{W}}{\mathrm{m^2}}\right) \times SA\left(\frac{\mathrm{W}}{\mathrm{m^2}}\right) - 0.02167\,H(\mathrm{m}) \times H(\mathrm{m}) \\ & + 0.00190\,TA(\mathrm{degree}) \times TA(\mathrm{degree}) + 0.000016\,P_o(\mathrm{W}) \\ & \times SA\left(\frac{\mathrm{W}}{\mathrm{m^2}}\right) + 0.000201\,P_o(W) \times H(m) + 0.000326\,P_o(\mathrm{W}) \\ & \times TA(\mathrm{degree}) - 0.000171\,SA\left(\frac{\mathrm{W}}{\mathrm{m^2}}\right) \times H(\mathrm{m}) \\ & + 0.000597\,SA\left(\frac{\mathrm{W}}{\mathrm{m^2}}\right) \times TA(\mathrm{degree}) - 0.0063\,H(\mathrm{m}) \\ & \times TA(\mathrm{degree}), \end{aligned} \tag{22}$$

$$\begin{aligned} P_H(\mathrm{kW}) = {} & 4.68 - 0.00098\,P_o(\mathrm{W}) - 0.00704\,SA\left(\frac{\mathrm{W}}{\mathrm{m^2}}\right) \\ & + 0.0328\,H(\mathrm{m}) - 0.0662\,TA(\mathrm{degree}) \\ & - 0.000000\,P_o(\mathrm{W}) \times P_o(\mathrm{W}) \\ & + 0.000003\,SA\left(\frac{\mathrm{W}}{\mathrm{m^2}}\right) \times SA\left(\frac{\mathrm{W}}{\mathrm{m^2}}\right) \\ & - 0.002173\,H(\mathrm{m}) \times H(\mathrm{m}) \\ & - 0.000571\,TA(\mathrm{degree}) \times TA(\mathrm{degree}) \\ & + 0.000001\,P_o(\mathrm{W}) \times SA\left(\frac{\mathrm{W}}{\mathrm{m^2}}\right) \\ & + 0.000024\,P_o(\mathrm{W}) \times H(\mathrm{m}) \\ & + 0.000017\,P_o(\mathrm{W}) \times TA(\mathrm{degree}) \\ & + 0000001\,SA\left(\frac{\mathrm{W}}{\mathrm{m^2}}\right) \times H(\mathrm{m}) \\ & + 0.000031\,SA\left(\frac{\mathrm{W}}{\mathrm{m^2}}\right) \times TA(\mathrm{degree}) \\ & - 0.000247\,H(\mathrm{m}) \times TA, \end{aligned} \tag{23}$$

$$\begin{aligned} \eta_{\mathrm{pump}} = {} & 118 - 0.0012 P_o(\mathrm{W}) - 0.321\,SA\left(\frac{\mathrm{W}}{\mathrm{m^2}}\right) + 0.78\,H(\mathrm{m}) \\ & - 2.42\,TA(\mathrm{degree}) - 0.000005\,P_o(\mathrm{W}) \times P_o(\mathrm{W}) \\ & + 0.000117\,SA\left(\frac{\mathrm{W}}{\mathrm{m^2}}\right) \times SA\left(\frac{\mathrm{W}}{\mathrm{m^2}}\right) - 0.0847\,H(\mathrm{m}) \times H(\mathrm{m}) \\ & - 0.0358\,TA(\mathrm{degree}) \times TA(\mathrm{degree}) + 0.000042\,P_o(\mathrm{W}) \\ & \times SA\left(\frac{\mathrm{W}}{\mathrm{m^2}}\right) + 0.001068\,P_o(\mathrm{W}) \times H(\mathrm{m}) + 0.000781\,P_o(\mathrm{W}) \\ & \times TA(\mathrm{degree}) + 0.00005\,SA\left(\frac{\mathrm{W}}{\mathrm{m^2}}\right) \times H(\mathrm{m}) + 0.00141\,SA\left(\frac{\mathrm{W}}{\mathrm{m^2}}\right) \\ & \times TA(\mathrm{degree}) - 0.0111\,H(\mathrm{m}) \times TA(\mathrm{degree}), \end{aligned} \tag{24}$$

$$\begin{aligned} \eta_{\mathrm{overall}} = {} & 37.9 - 0.0075\,P_o(\mathrm{W}) - 0.0660\,SA\left(\frac{\mathrm{W}}{\mathrm{m^2}}\right) + 0.336\,H(\mathrm{m}) \\ & - 0.645\,TA(\mathrm{degree}) - 0.000 P_o(\mathrm{W}) \times P_o(\mathrm{W}) \\ & + 0.000023\,SA\left(\frac{\mathrm{W}}{\mathrm{m^2}}\right) \times SA\left(\frac{\mathrm{W}}{\mathrm{m^2}}\right) - 0.02107\,H(\mathrm{m}) \times H(\mathrm{m}) \\ & - 0.00288\,TA(\mathrm{degree}) \times TA(\mathrm{degree}) + 0.000009\,P_o(\mathrm{W}) \\ & \times SA\left(\frac{\mathrm{W}}{\mathrm{m^2}}\right) + 0.000224\,P_o(\mathrm{W}) \times H(\mathrm{m}) + 0.00164 P_o(\mathrm{W}) \\ & \times TA(\mathrm{degree}) + 0.000010\,SA\left(\frac{\mathrm{W}}{\mathrm{m^2}}\right) \times H(\mathrm{m}) \\ & + 0.00295\,SA\left(\frac{\mathrm{W}}{\mathrm{m^2}}\right) \times TA(\mathrm{degree}) - 0.00233\,H(\mathrm{m}) \\ & \times TA(\mathrm{degree}), \end{aligned} \tag{25}$$

TABLE 4 The coded level of input factors.

Parameters	Unit	Coded value −2	−1	0	1	2
PV power output (P_o)	W	4000	4250	4500	4750	5000
Solar radiation (SA)	W/m^2	200	350	500	650	800
Operating head (H)	m	15	20	25	30	35
Tilt angle (TA)	degree	5	10	15	20	25

TABLE 5 Experimental design matrix.

Exp. Run	P_o (W)	SA (W/m^2)	Head (m)	TA (degree)	Discharge, Q (m^3/h)	Hydraulic power (kW)	Pump efficiency (%)	Overall efficiency (%)
1	4500	500	25	15	20.4	1.57	68.33	13.35
2	4750	350	20	10	20.64	1.31	56.63	10.89
3	4500	500	15	15	21.6	1.08	47.99	8.65
4	4500	500	25	5	21.42	1.49	55.21	11.12
5	4750	350	30	10	18.6	1.70	74.10	14.56
6	4250	650	30	20	17.64	1.62	70.64	13.83
7	4750	350	30	20	18.99	1.73	75.53	14.86
8	4500	500	25	15	20.4	1.57	68.33	13.35
9	4750	350	20	20	22.47	1.41	61.05	11.82
10	4250	350	30	20	17.07	1.58	68.60	13.41
11	4250	650	30	10	17.37	1.60	69.69	13.63
12	5000	500	25	15	21.74	1.66	69.32	14.20
13	4250	350	20	20	20.18	1.29	55.54	10.66
14	4500	500	25	25	20.49	1.58	75.21	15.42
15	4500	500	25	15	20.4	1.57	68.33	13.35
16	4750	650	20	10	23.41	1.46	63.30	12.29
17	4250	650	20	10	20.64	1.31	56.63	10.89
18	4500	500	35	15	15.6	1.67	72.66	14.26
19	4250	350	30	10	16.65	1.54	67.09	13.09
20	4500	800	25	15	24	1.81	79.16	15.62
21	4000	500	25	15	19.47	1.51	65.55	12.77
22	4250	650	20	20	22.93	1.44	62.15	12.05
23	4750	650	20	20	26.77	1.64	71.39	13.99
24	4500	500	25	15	20.4	1.57	68.33	13.35
25	4250	350	20	10	23.84	1.48	64.34	12.51
26	4500	500	25	15	20.4	1.57	68.33	13.35
27	4750	650	30	10	20.31	1.84	80.30	15.86
28	4500	500	25	15	20.4	1.57	68.33	13.35
29	4500	500	25	15	20.4	1.57	68.33	13.35
30	4500	200	25	15	24.13	1.82	79.56	15.71
31	4750	650	30	20	20.55	1.86	81.17	16.05

After 31 different lab tests were completed, the model's fitness and surface plot were analyzed. To characterize the responses and their impact on the input elements, three-dimensional surface plots were used as illustrations. The experiment verified the outcome.

The Pareto plots used to find interaction effects of input on output response. Using Pareto plots it is easy to find key input factor which is responsible for specified output response. It displays the absolute values of the effects, and draws a reference line on the chart. Any effect that extends past this reference line is potentially

TABLE 6 ANOVA results of discharge and hydraulic power.

		Discharge, Q (m^3/h)				Hydraulic power (kW)			
Source	DF	Adj SS	Adj MS	*F*-Value	*P*-Value	Adj SS	Adj MS	*F*-Value	*P*-Value
Model	14	153.212	10.9437	8.85	0.000	0.824441	0.058889	18.44	0.000
Linear	4	108.964	27.2411	22.03	0.000	0.569485	0.142371	44.58	0.000
P_o (W)	1	16.593	16.5934	13.42	0.002	0.080040	0.080040	25.06	0.000
SA (W/m^2)	1	4.958	4.9577	4.01	0.062	0.020466	0.020466	6.41	0.022
H (m)	1	86.959	86.9595	70.33	0.000	0.458725	0.458725	143.63	0.000
TA (degree)	1	0.454	0.4537	0.37	0.553	0.010254	0.010254	3.21	0.092
Square	4	31.060	7.7650	6.28	0.003	0.204307	0.051077	15.99	0.000
P_o (W)*P_o (W)	1	0.044	0.0443	0.04	0.852	0.000016	0.000016	0.01	0.944
SA (W/m^2)*SA (W/m^2)	1	19.445	19.4453	15.73	0.001	0.092674	0.092674	29.02	0.000
H (m)*H (m)	1	8.397	8.3965	6.79	0.019	0.084412	0.084412	26.43	0.000
TA (degree)*TA (degree)	1	0.065	0.0649	0.05	0.822	0.005826	0.005826	1.82	0.196
2-Way interaction	6	13.187	2.1979	1.78	0.167	0.050649	0.008441	2.64	0.056
P_o (W)*SA (W/m^2)	1	5.660	5.6596	4.58	0.048	0.019701	0.019701	6.17	0.024
P_o (W)*H (m)	1	1.010	1.0100	0.82	0.379	0.014059	0.014059	4.40	0.052
P_o (W)*TA (degree)	1	2.654	2.6536	2.15	0.162	0.007514	0.007514	2.35	0.145
SA (W/m^2)*H (m)	1	0.263	0.2632	0.21	0.651	0.000009	0.000009	0.00	0.958
SA (W/m^2)*TA (degree)	1	3.208	3.2077	2.59	0.127	0.008756	0.008756	2.74	0.117
H (m)*TA (degree)	1	0.393	0.3931	0.32	0.581	0.000609	0.000609	0.19	0.668
Error	16	19.782	1.2364	–	–	0.051101	0.003194	–	–
Lack-of-fit	10	19.782	1.9782	–	–	0.051101	0.005110	–	–
Modal									
SD (Standard deviation)		1.11193				0.0565136			
R^2		88.56%				94.16%			
Adjusted R^2		78.56%				89.06%			
Predicted R^2		34.13%				66.38%			

important. From this figure, it was seen that PV power output play more important role for all output responses. Solar radiation seems to be next input variable effect the all output responses. Minitab displays the absolute value of the standardized effects of factors when there is an error term.

Figure 4 represents the Pareto chart and residual plot of ANOVA regression analysis. The Pareto chart shows the standardized effect of control variables (Solar PV output power, solar radiation, water head, and tilt angle) on the response variable.

3.3 | RSM optimizer

Figure 5 illustrates how the RSM optimizer was utilized to determine the ideal input process parameters at which the best potential output responses were available. The different output factor weightages used for the multi-objective optimization. The purpose of this effort is to improve solar PV water pump performance by optimizing the input variables PV power output, SA, operating head, and TA.

In accordance with RSM, the ideal process parameters for P_o, SA, Head, and TA were discovered to be 5000 W, 260 W/m^2, 35 m, and 19°, respectively. The optimal settings were determined to be 16.8 m^3/h discharge, 1.85 kW hydraulic power, 81.15% pump efficiency, and 16.12% overall efficiency at the aforementioned level. All replies show a desire for unity, which is a favorable sign of process optimization of the solar pump's performance by use of the RSM technique. In optimization research, a desirability value near 1 denotes an optimum answer. The desirability value of 0.9693 in our investigation indicates that there is an acceptable range.

4 | RESULT AND DISCUSSIONS

The experimental design technique was used in this work to alter the operating parameters in order to improve the efficiency of the solar PV water pump. A 3-D surface plot is used to show how these altered circumstances interact with one another. In this plot, two variables vary at a time and the other two variables keep hold. In this section, the impact of the control factor on P_o, SA, head, and TA is discussed.

TABLE 7 ANOVA results of pump efficiency and overall efficiency.

		Pump efficiency (%)				Overall efficiency (%)			
Source	DF	Adj SS	Adj MS	*F*-Value	*P*-Value	Adj SS	Adj MS	*F*-Value	*P*-Value
Model	14	1673.87	119.562	9.48	0.000	78.0303	5.5736	9.88	0.000
Linear	4	1176.41	294.102	23.33	0.000	55.6069	13.9017	24.64	0.000
P_o (W)	1	132.29	132.289	10.49	0.005	7.1661	7.1661	12.70	0.003
SA (W/m^2)	1	41.55	41.550	3.30	0.088	1.8323	1.8323	3.25	0.090
H (m)	1	881.17	881.172	69.90	0.000	41.0700	41.0700	72.80	0.000
TA (degree)	1	121.40	121.397	9.63	0.007	5.5384	5.5384	9.82	0.006
Square	4	394.64	98.659	7.83	0.001	17.8889	4.4722	7.93	0.001
P_o (W)*P_o (W)	1	3.30	3.301	0.26	0.616	0.0111	0.0111	0.02	0.890
SA (W/m^2)*SA (W/m^2)	1	199.41	199.405	15.82	0.001	7.9133	7.9133	14.03	0.002
H (m)*H (m)	1	128.21	128.215	10.17	0.006	7.9327	7.9327	14.06	0.002
TA (degree)*TA (degree)	1	22.90	22.899	1.82	0.197	0.1483	0.1483	0.26	0.615
2-Way Interaction	6	102.83	17.138	1.36	0.289	4.5346	0.7558	1.34	0.297
P_o (W)*SA (W/m^2)	1	40.00	39.997	3.17	0.094	1.7639	1.7639	3.13	0.096
P_o (W)*H (m)	1	28.54	28.542	2.26	0.152	1.2587	1.2587	2.23	0.155
P_o (W)*TA (degree)	1	15.26	15.255	1.21	0.288	0.6728	0.6728	1.19	0.291
SA (W/m^2)*H (m)	1	0.02	0.019	0.00	0.970	0.0008	0.0008	0.00	0.970
SA (W/m^2)*TA (degree)	1	17.78	17.777	1.41	0.252	0.7839	0.7839	1.39	0.256
H (m)*TA (degree)	1	1.24	1.236	0.10	0.758	0.0545	0.0545	0.10	0.760
Error	16	201.69	12.606	–	–	9.0258	0.5641	–	–
Lack-of-fit	10	201.69	20.169	–	–	9.0258	0.9026	–	–
Modal									
SD (Standard deviation)		3.55044				0.751074			
R^2		89.25%				89.63%			
Adjusted R^2		79.84%				80.56%			
Predicted R^2		38.06%				40.28%			

4.1 | Impact of control factors on discharge (Q) through the solar pump

The discharge of the solar water pump is the amount of water released per unit time. The cumulative effect of input parameters on the discharge through the pump is shown in Figure 4. Figure 4a shows the effect of PV output power and solar radiation on the discharge of the solar pump and the other two variables are kept on hold. It was noticed that when the power output of the PV array increased, the amount of water discharged by the pump increases as well, reaching its maximum discharge at 4750 W PV power. The discharge value rises together with the solar radiation because as solar radiation gets stronger, PV cells create more current, which powers the pump more effectively. As a result, discharge is greatest at midday, especially during the summer when the sun's intensity is at its peak.[20]

Figure 6b illustrates the effect of SA and the operating head while maintaining the other two variables constant. It has been shown that the discharge is inversely related to operating head since it is lowest at the highest operating head. This is because increasing the working head requires more energy to provide the water, which is overcome by decreasing the amount of outflow. Figure 6c illustrates how the tilt angle affects the discharge and shows that as the tilt angle increases, more solar radiation reaches the solar panel, supplying more power to the pump.

4.2 | Impact of control factors on hydraulic power (P_H)

Basically, the power developed by the pump to supply the water is termed the hydraulic power of the pump. It is mainly dependent on the discharge and head of the pump. Figure 5 depicts the iterative effect of input attributes on the hydraulic power of the pump. Figure 5a shows how the P_H improves along with the PV array power and reaches its maximum output at 5000 W. The P_H increases with solar radiation and has reached a maximum. This is so that more energy may be produced by the panel and pump when solar radiation rises. As a result, the P_H varies depending on the day time and season.

Figure 7b depicts the variation of SA and head and the other two parameters kept at hold. As the P_H is heavily reliant on the operating

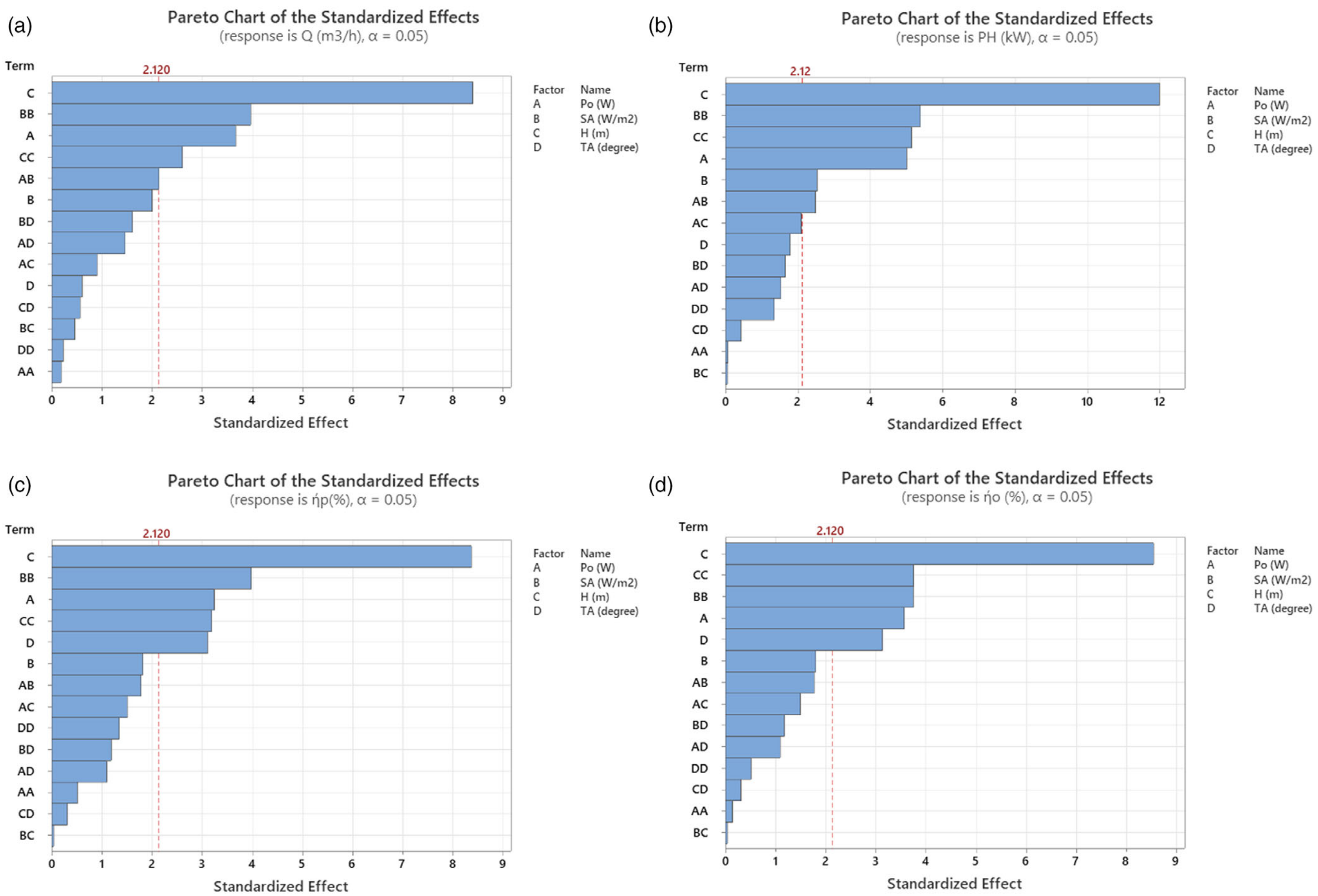

FIGURE 4 Pareto plot and residual plot of output response regression model.

head, it has been noticed that it rises with working head and reaches its maximum at 35 m head.[19] Figure 7c shows that the tilt angle increases hydraulic power because it allows the PV array to receive more solar radiation, which increases power production.

4.3 | Impact of control factors on pump efficiency ($ή_p$)

The efficiency of a pump is defined by how successfully it can convert one kind of energy to another depending on the difference in hydraulic power going into and out of the pump. The cumulative effect of all input factors on the pump efficiency is described in Figure 8. It was determined that when P_o increased, pump efficiency increased until the pump achieved its maximum power. Also, the surface plot revealed that when the solar radiation rises, the pump efficiency of solar PV water pump system rises as well. This is because when the radiation raises, the photovoltaic cell charges more and provides more power to the solar pump.

The pump efficiency of the PV solar pump is influenced by the solar intensity and operating head as shown in Figure 8b where the other two variables are kept on hold. As operating head increases, the solar pump's pump efficiency increases, forcing the components to operate near to or at their rated conditions and resulting in increased efficiencies. Performance of a PV system is significantly influenced by its tilt angle with respect to the horizontal. This is because, as seen in Figure 8c, the quantity of solar energy that the PV panel gets changes as a result of variations in tilt angle. The tilt angle was shown to have a considerable impact on the instantaneous photovoltaic production, increasing the effectiveness of the solar PV water pump.[31]

4.4 | Impact of control factors on overall efficiency ($ή_o$)

Figure 9 depicts the effect of various input parameters on the overall efficiency. The 3D surface plot shows how different variables impact the overall efficiency. Figure 9a illustrates the impact of P_o and SA on the overall efficiency while holding the value of head and TA. It was discovered that when the PV array provided more power for the solar pump, total efficiency increased as the PV power output increased. With an increase in solar radiation, the PV solar pump's efficiency likewise increases ([32–34]).

Figure 9b illustrates the variation of SA and head on the overall efficiency and found that it increases with the operating head and reaches maximum efficiency at 35 m operating head.[33] It was also

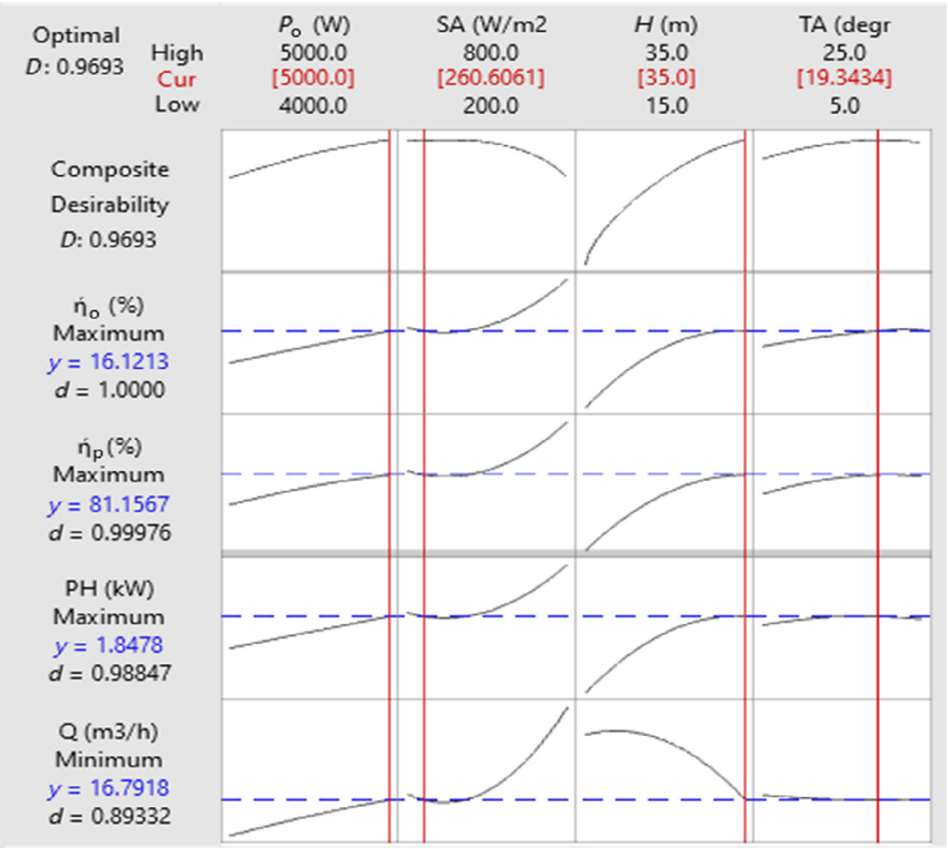

FIGURE 5 Optimization plot: Effect of process parameters on responses.

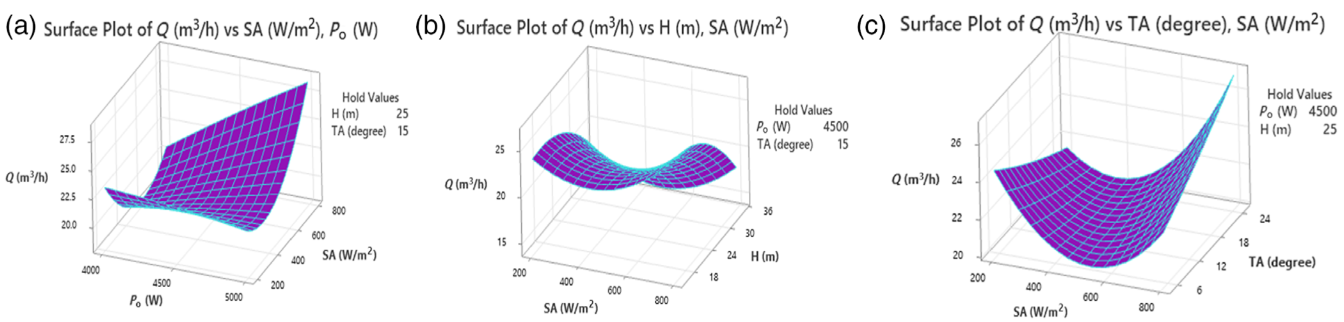

FIGURE 6 Effect of process parameter on discharge (m^3/h).

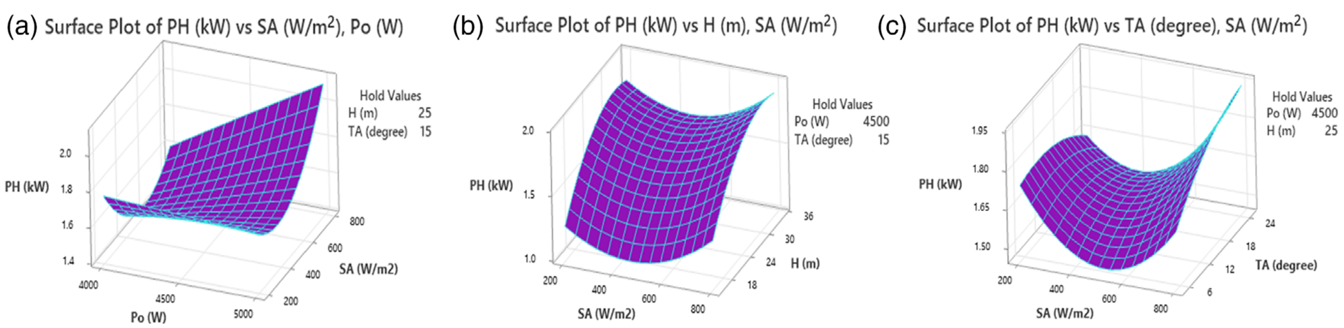

FIGURE 7 Effect of process parameter on hydraulic power (kW).

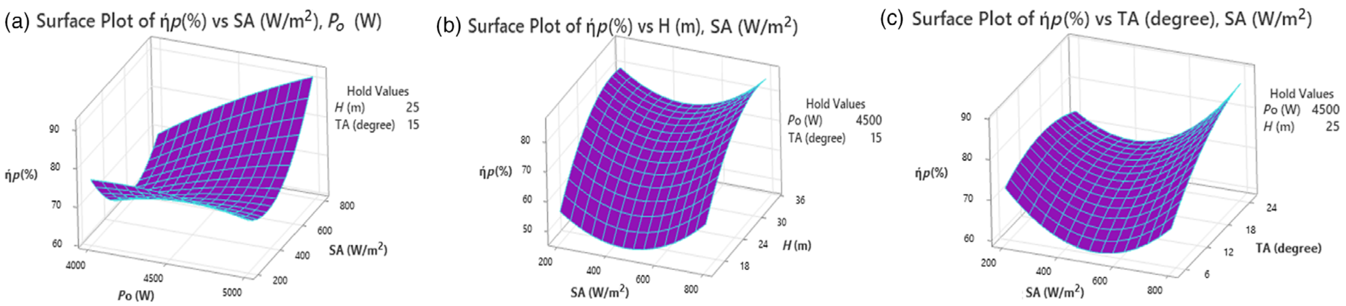

FIGURE 8 Effect of process parameter on pump efficiency (%).

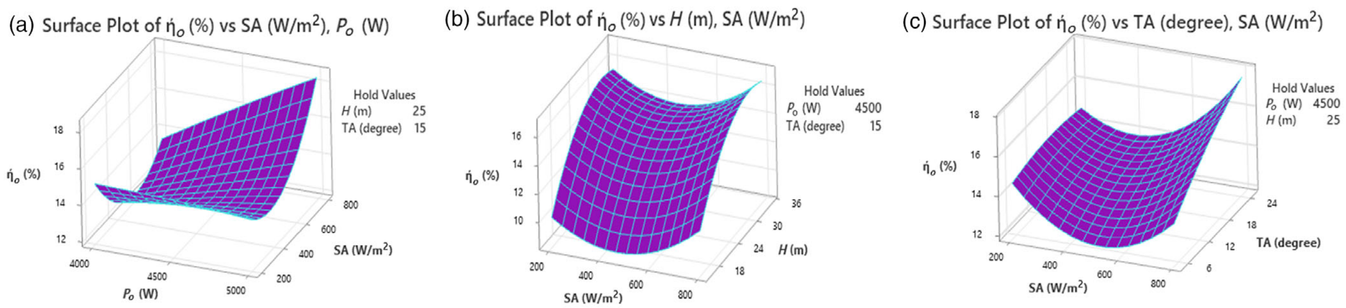

FIGURE 9 Effect of process parameter on overall efficiency (%).

TABLE 8 Validation of model result.

Output response	Predicted value	Tested value	Error (%)
Discharge (m^3/h)	16.8	17.10	1.8
Hydraulic power (kW)	1.85	1.81	2
Pump efficiency (%)	81.15	78.55	3.2
Overall efficiency (%)	16.12	15.67	2.8

Note: Optimal value: 5000 W P_o, 260 W/m^2 SA, 35 m Head, and 19° TA.

observed from Figure 9c that the efficiency of the solar water pump is higher in the winter season than in summer season since higher tilt angle of the solar panel maintained in winter. The higher Solar panel temperature also reduced the solar panel efficiency drastically.[34]

5 | CONFIRMATION TEST

Even though an acceptable desirability value was achieved, it was thought necessary to run a validation test to ensure the study's reliability. In this validation investigation, the optimal operating parameters acquired via optimization were used in an experimental study, and the outcomes were compared. Table 8 shows that the percentage of error in the estimate of the created models was within acceptable bounds. It was found the error % for discharge, hydraulic power, pump efficiency, and overall efficiency are 1.8%, 2%, 3.2%, and 2.8% respectively.

The percentage error in the prediction of constructed models was found to be in good accord. The validation of data revealed that the constructed models were highly accurate, with the proportion of error in prediction being in good accord. The optimization research was deemed effective since the error rates disclosed in this verification investigation were less than 5%, as indicated in Table 8.

6 | CONCLUSIONS

In this work, an attempt was made to identify the optimal performance of a solar photovoltaic water pump, and the impacts of PV power output, solar radiation, operating head, and tilt angle on PV water pump performance were explored using the RSM model. According to the ANOVA analysis, all of the created models give a good match. The following conclusions were obtained in this investigation:

- The input factors and the response can be related, according to the response surface approach. RSM was utilized to approximation the experimental and the numerical responses using several statistical, graphical, and mathematical methodologies.
- According to the RSM, the optimal process parameters for P_o, SA, Head, and TA are 5000 W, 260 W/m^2, 35 m, and 19°, respectively. At the aforementioned level, the ideal parameters were determined to be 16.8 m^3/h discharge, 1.85 kW hydraulic power, 81.15% pump efficiency, and 16.12% overall efficiency.

- The desirability value was calculated to be 0.9693. The R^2 value for discharge, hydraulic power, pump efficiency, and overall efficiency was 88.56%, 94.16%, 89.25%, and 89.63, respectively, which indicates that the model is successful.
- Also, from the ANOVA findings it was conclude that PV power output (P_o) and head (H) has significant effect on the output response and maximum efficiency is found when the solar radiation (SA) is maximum.
- It was also found the error % for discharge, hydraulic power, pump efficiency, and overall efficiency are 1.8%, 2%, 3.2%, and 2.8% respectively. The optimization research was deemed effective since the error rates disclosed in this verification investigation were less than 5%. The high cost, lengthy, and labor-intensive experimental technique may be overcome with the help of the optimization research.
- The DoE design and ANOVA findings are given in this article show that discharge and operating head have a substantial impact on the pump's hydraulic power. Numerous concerns have arisen as a result of this work, including the impacts of ambient temperature, surface azimuthal angle, motor speed, and PV array size.

NOMENCLATURE

ANOVA	analysis of variance
DoE	design of expert
H	operating head (m)
P_H	hydraulic power (kW)
P_o	PV array power output (W)
PV	photovoltaic
Q	discharge (m^3/h)
RSM	response surface methodology
SA	solar radiation (W/m^2)
SPVWPS	solar photovoltaic water pump system
TA	tilt angle (degree)

AUTHOR CONTRIBUTIONS

Vipan Chand Waila: Conceptualization; investigation; methodology. **Abhishek Sharma:** Conceptualization; formal analysis; supervision. **Vineet Singh**: Investigation, Methodology. **Naveen Kumar Gupta**: Final Draft, formal analysis and methodology

DATA AVAILABILITY STATEMENT

The data that support the findings of this study are available from the corresponding author upon reasonable request.

ORCID

Abhishek Sharma https://orcid.org/0000-0001-9189-2902

REFERENCES

1. Anjum S, Mukherjee V. A novel arithmetic sequence pattern reconfiguration technique for line loss reduction of photovoltaic array under non-uniform irradiance. *J Clean Prod*. 2022;10(331):129822.
2. Chahartaghi M, Nikzad A. Exergy, environmental, and performance evaluations of a solar water pump system. *Sustain Energy Technol Assess*. 2021;1(43):100933.
3. Lin MH, Lin JH, El Haj AM, Alayi R, Seyednouri SR. Optimal location and sizing of wind turbines and photovoltaic cells in the grid for load supply using improved genetic algorithm. journal of renewable. *Energy Environ*. 2022;10(2):1-10. doi:10.30501/jree.2022.327250.1321
4. Shaikh A, Shaikh PH, Kumar L, et al. Design and modeling of a grid-connected PV–WT hybrid microgrid system using net metering facility. *Iran J Sci Technol, Trans Electr Eng*. 2022;46(4):1189-1205. doi:10.1007/s40998-022-00530-4
5. Prakash O, Ahmad A, Kumar A, et al. The compressive study of energy security prospects in India through solar power. *Int J Low-Carbon Technol*. 2022;8(17):962-979. doi:10.1093/ijlct/ctac075
6. Jahangiri M, Raeiszadeh F, Alayi R, Najafi A, Tahmasebi A. Development of rural tourism in Iran using PV-based system: finding the best economic configuration. *J Renew Energy Environ*. 2022;9(4):1-9. doi:10.30501/jree.2022.298089.1234
7. Anjum S, Khan MA, Bodha KD, Ahluwalia D. Modeling and experimental validation of matrix structure photovoltaic array reconfiguration technique to harvest maximum power under continuous dynamic shading condition. *Optik*. 2022;1(271):170141.
8. Aldawoud A, Aldawoud A, Aryanfar Y, Assad ME, Sharma S, Alayi R. Reducing PV soiling and condensation using hydrophobic coating with brush and controllable curtains. *Int J Low-Carbon Technol*. 2022;8(17):919-930.
9. Chilundo RJ, Mahanjane US, Neves D. Design and performance of photovoltaic water pumping systems: comprehensive review towards a renewable strategy for Mozambique. *J Power Energy Eng*. 2018;6(7):32-63.
10. Singh B, Sharma U, Kumar S. Standalone photovoltaic water pumping system using induction motor drive with reduced sensors. *IEEE Trans Ind Appl*. 2018;54(4):3645-3655.
11. Benghanem M, Daffallah KO, Almohammedi A. Estimation of daily flow rate of photovoltaic water pumping systems using solar radiation data. *Results Phys*. 2018 Mar;1(8):949-954.
12. Muralidhar K, Rajasekar N. A review of various components of solar water-pumping system: configuration, characteristics, and performance. *Int Trans Electr Energy Syst*. 2021;31(9):e13002.
13. Errouha M, Derouich A, Nahid-Mobarakeh B, Motahhir S, El Ghzizal A. Improvement control of photovoltaic based water pumping system without energy storage. *Solar Energy*. 2019;15(190):319-328.
14. de Oliveira FA, Brito AU, Galhardo MA, Ferreira L, Macêdo WN. Modeling, control and simulation of a small photovoltaic-wind water pumping system without battery bank. *Comp Electr Eng*. 2020;1(84):106619.
15. Errouha M, Motahhir S, Combe Q, Derouich A, El Ghzizal A. Fuzzy-PI controller for photovoltaic water pumping systems. *2019 7th international renewable and sustainable energy conference (IRSEC) 2019, November 27*. IEEE; 2019;1-6.
16. Allouhi A, Buker MS, El-Houari H, et al. PV water pumping systems for domestic uses in remote areas: sizing process, simulation and economic evaluation. *Renew Energy*. 2019;1(132):798-812.
17. Errouha M, Derouich A, El Ouanjli N, Motahhir S. High-performance standalone photovoltaic water pumping system using induction motor. *Int J Photoenergy*. 2020;18(2020):1-3.
18. Kumar SS, Bibin C, Akash K, Aravindan K, Kishore M, Magesh G. Solar powered water pumping systems for irrigation: a comprehensive review on developments and prospects towards a green energy approach. *Mater Today: Proc*. 2020;1(33):303-307.
19. Verma S, Mishra S, Chowdhury S, et al. Solar PV powered water pumping system–a review. *Mater Today: Proc*. 2021 Jan;1(46):5601-5606.
20. Tiwari AK, Kalamkar VR. Effects of total head and solar radiation on the performance of solar water pumping system. *Renew Energy*. 2018 Apr;1(118):919-927.

21. Abhilash P, Kumar RN, Kumar RP. Solar powered water pump with single axis tracking system for irrigation purpose. *Mater Today: Proc*. 2021;1(39):553-557.
22. Tomar A. A cooperative irrigation based PV water pumping system with enhanced PV utilization. *2021 IEEE 2nd International Conference on Smart Technologies for Power, Energy and Control (STPEC), December 19*. IEEE; 2021;1-5.
23. Chand WV, Sharma A, Yusuf M. Optimizing the performance of solar PV water pump by using response surface methodology. *EVERGREEN Joint Journal of Novel Carbon Resource Sciences & Green Asia Strategy*. 2022;9:1151-1159.
24. Sharma R, Sharma S, Tiwari S. Design optimization of solar PV water pumping system. *Mater Today: Proc*. 2020;1(21):1673-1679.
25. Yang Y, Li X, Gu Y, et al. Adsorption property of fluoride in water by metal organic framework: optimization of the process by response surface methodology technique. *Surf Interfaces*. 2022;1(28):101649.
26. Kumar M, Ansari NA, Sharma A, Singh VK, Gautam R, Singh Y. Prediction of an optimum engine response based on different input parameters on common rail direct injection diesel engine: a response surface methodology approach. *Scient Iran*. 2021;28(6):200-3181.
27. Elkelawy M, El Shenawy EA, Bastawissi HA, Shams MM, Panchal H. A comprehensive review on the effects of diesel/biofuel blends with nanofluid additives on compression ignition engine by response surface methodology. *Energy Convers Manage: X*. 2022;17:100177.
28. Kumar M, Singh VK, Sharma A, Ansari NA, Gautam R, Singh Y. Effect of fuel injection pressure and EGR techniques on various engine performance and emission characteristics on a CRDI diesel engine when run with linseed oil methyl ester. *Energy Environ*. 2022;33(1):41-63.
29. Sharma A, Pali HS, Kumar M, Singh NK, Singh Y, Singh D. Study the effect of optimized input parameters on a CRDI diesel engine running with waste frying oil methyl ester-diesel blend fuel with ZnO nanoparticles: a response surface methodology approach. *Biomass Convers Bioref*. 2022;28:1-26.
30. Singh A, Sinha S, Choudhary AK, Panchal H, Elkelawy M, Sadasivuni KK. Optimization of performance and emission characteristics of CI engine fueled with Jatropha biodiesel produced using a heterogeneous catalyst (CaO). *Fuel*. 2020;15(280):118611.
31. Kahveci EE, Taymaz I. Hydrogen PEMFC stack performance analysis through experimental study of operating parameters by using response surface methodology (RSM). *Int J Hydrogen Energy*. 2022;47(24):12293-12303.
32. Vishnupriyan J, Partheeban P, Dhanasekaran A, Shiva M. Analysis of tilt angle variation in solar photovoltaic water pumping system. *Mater Today: Proc*. 2022;1(58):416-421.
33. Fouda TZ, Derbala AA, Elmetwalli AH, Elbelkemy AA. Evaluation of photovoltaic solar-powered water pumping irrigation system during winter season. *MISR J Agric Eng*. 2018;35(1):91-104.
34. Singh V, Yadav VS. Application of RSM to optimize solar pump LCOE and power output. *IETE J Res*. 2022;64:10-12.

How to cite this article: Waila VC, Sharma A, Singh V, Gupta NK. Solar photovoltaic water pump performance optimization by using response surface methodology. *Environ Prog Sustainable Energy*. 2023;e14148. doi:10.1002/ep.14148